9th Asia-Pacific Conference on Wind Engineering
Auckland, New Zealand
3-7 December 2017

Rain load for transmission tower-line system

Xing Fu[1], Hong-Nan Li[1]

[1]Faculty of Infrastructure Engineering
Dalian University of Technology, Dalian 116023, China

Abstract

Rain load has great impact on the response of transmission tower-line system based on previous research. This paper introduces the calculating methodology of rain load for transmission tower and transmission line at first, and then the wind tunnel test is carried out to validate the effectiveness of the proposed rain load model. According to both the numerical and experimental results, it can be found that rain load has significant effect on the response of transmission tower-line system and should be given more attention.

Introduction

During a typhoon or hurricane, the strong wind is usually accompanied with heavy rainfalls, while the forming mechanism of rain load is still not clear. Historically, numerous structures have collapsed during severe gales and thunderstorms. Most of the time, researchers have attributed the collapses to strong winds [7]. The effect of rainfall on building physics has attracted lots of attentions [1], and yet its effect on the dynamic response of structures has been ignored in design. Thus, it is necessary to study the rain load model and reveal its acting mechanism.

Some researchers studied the rain load on tall structures. Li et al. [10] proposed an approach for the rain load on the transmission tower, and carried out the dynamic response analyses and experiments of transmission tower under the wind and rain loads. Their results showed that the proposed approach agreed well with the wind tunnel test and the rain load influence on the transmission towers should not be ignored for strong rainstorms. Fu et al. [8] modified the rain load model proposed by Li et al. [10] and the wind tunnel test revealed that the rain load could not be neglected during severe gales and thunderstorms. By simulating the motion of a single raindrop, Fu et al. [7] validated and explained the phenomenon that the horizontal velocity of raindrop was larger than the corresponding wind speed, and then the velocity difference was introduced to further modify the rain load formula.

For the transmission conductor, one of the most important tasks is to measure the aerodynamic properties which are used to calculate the wind load acting on it. Wardlaw et al. [12] have measured the mean force acting on bundled conductors based on wind tunnel test, and the relationship of drag coefficient and Reynolds number were provided. Tabatabai et al. [11] studied the drag properties of trapezoidal and circular wire conductors, and indicated that, at high wind speeds, the trapezoidal wire conductors had lower drag coefficients than comparable standard circular wire conductors due to the smooth surface of trapezoidal conductor. Kikuchi et al. [9] measured the drag properties of the LP conductor under both wind and rain excitations, and the experimental results revealed that the influence of heavy rainfall is not negligible on the new-design wire. Xie et al. [13] observed the global drag coefficients of multi-bundled conductors with the wind tunnel test, and showed that the global drag coefficients of multi-bundled conductors were much smaller than those of a single conductor in the same wind velocity with any attack angle and the biggest global drag coefficients corresponding to different conditions investigated in this study are less than those recommended in the design codes worldwide.

Based on the abovementioned research studies, it can be seen that some pioneering work of rain load on transmission tower has been performed. However, the research of rain load still needs to be continued.

Single raindrop impinging force

To measure the single raindrop impinging force, a piezoelectric transducer is designed and fabricated, as shown in Figure 1. After that the calibration test was conducted and the results showed goog linear relationship. Figure 2 shows the experimental equipment, and the air level is used to make the transducer surface remain level.

A simple calibration method is presented based on the Newton's second law. After the calibration, the magnitudes of input and output sine waves are obtained, and then the curve of calculated inertia force and the output voltage is illustrated in Figure 3, which indicating that the raw data have a good linear relationship.

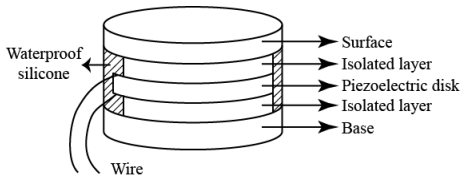

Figure 1 Piezoelectric transducer

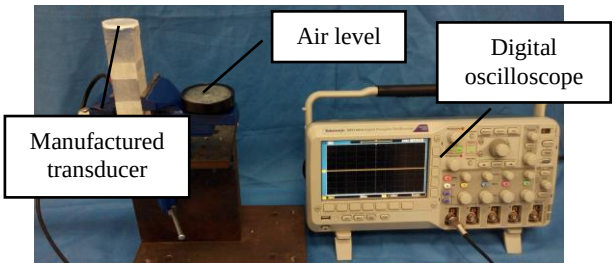

Figure 2 The experimental equipment

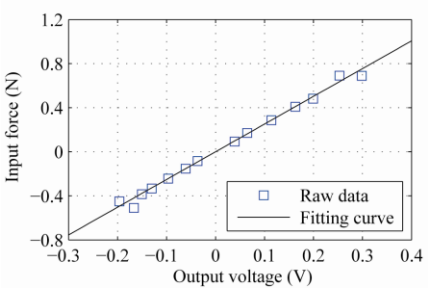

Figure 3 The calculated input force vs. the output voltage

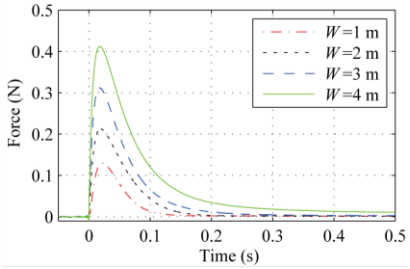

Figure 4 Average curves of raindrop impinging force vs. time for different release heights

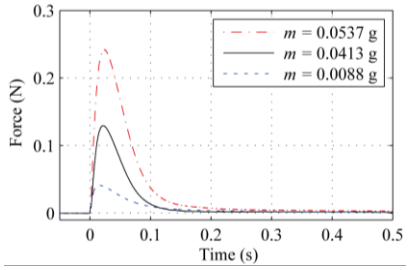

Figure 5 Average curves of raindrop impinging force vs. time for different raindrop masses

The average time history curves of the raindrop impinging force with different release heights and raindrop masses are given in Figure 4 and Figure 5 respectively.

The trajectory of a raindrop can be simulated by the following equations [2]:

$$m\frac{\mathrm{d}^2x}{\mathrm{d}t^2}=3\pi\mu D(V_x-\frac{\mathrm{d}x}{\mathrm{d}t})\frac{C_DRe}{24} \tag{1}$$

$$m\frac{\mathrm{d}^2y}{\mathrm{d}t^2}=3\pi\mu D(V_y-\frac{\mathrm{d}y}{\mathrm{d}t})\frac{C_DRe}{24} \tag{2}$$

$$m\frac{\mathrm{d}^2z}{\mathrm{d}t^2}=3\pi\mu D(V_z-\frac{\mathrm{d}z}{\mathrm{d}t})\frac{C_DRe}{24}-mg(1-\frac{\rho_a}{\rho_w}) \tag{3}$$

where m is the raindrop mass; C_D is the drag coefficient; Re is Reynolds number; μ is the air viscosity; ρ_w is the raindrop density; D is the raindrop diameter; V_x, V_y and V_z are the wind velocity components in the x, y and z directions.

With the calculated impact velocity, the peak force for each curve in Figure 4 and Figure 5 are captured, and can be fitted by the following formula:

$$F_{peak}(V,D)=k\rho_wV^2D^3 \tag{4}$$

where k takes 102.0 in 1/m and V is the raindrop velocity before impinging on the target surface.

The raindrop impinging force curves in Figure 4 and Figure 5 are normalized by dividing the forces by F_{peak}, of which the resulting normalized curves are illustrated in Figure 6. In addition, the average curve of the six normalized curves is also calculated and shown in Figure 6. As can be seen, the peak value of the average normalized curve is unity. With the fitting formula of peak force and average normalized curve made available, the predicted time history curve of raindrop impinging force can be easily obtained for various combinations of impinging velocity and raindrop mass.

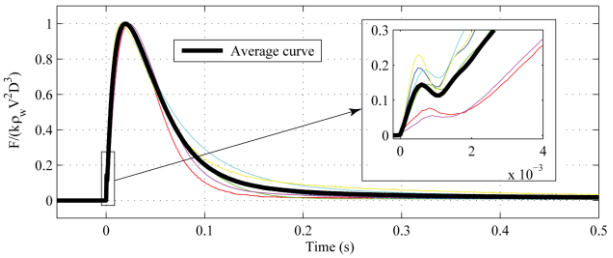

Figure 6 The normalized curves for raindrop impinging force

Rain load for transmission tower and validation

The raindrop size distribution, indicating the number of droplets with a specified diameter in the unit volume of air, can be simulated using the M-P spectra:

$$n(D,R)=n_0\exp(-\Lambda D) \tag{5}$$

where $n_0=8\times10^3$ in $1/(\mathrm{m}^3\cdot\mathrm{mm})$, $\Lambda=4.1R^{-0.21}$ in 1/mm, and R is the rain intensity in mm/h.

First, the mean wind speed as a function of altitude can be described by the following power-law wind speed profile:

$$V_a(V_{10},H,\alpha)=V_{10}\left(\frac{H}{10}\right)^{\alpha} \tag{6}$$

where V_{10} is the basic wind speed representing the mean wind speed during 10 min at the altitude of 10 m, H is the altitude, and α is the power-law exponent.

The velocity of a raindrop is larger than the corresponding wind speed in the horizontal direction [3] and this phenomenon can be quantified by the velocity ratio. The ratio is defined as the ratio of raindrop horizontal velocity to the corresponding wind speed, which can be expressed as [7]

$$\gamma(H,D,\alpha)=\left(0.2373H^{-0.5008}-0.0167\right)\left(\frac{D}{3}\right)^{0.8}\left(\frac{\alpha}{0.12}\right)+1 \tag{7}$$

A schematic of the raindrop distribution is shown in Figure 7, and the time interval between two adjacent raindrops is:

$$\Delta t(V_r,R)=\frac{\sqrt{2}l}{V_r}=\frac{\sqrt{2}}{\sqrt[3]{N(R)}V_r} \tag{8}$$

where V_r is the raindrop velocity; $N(R)$ is the total number of raindrops per unit volume taking $\int_0^{\infty}n(D,R)dD$.

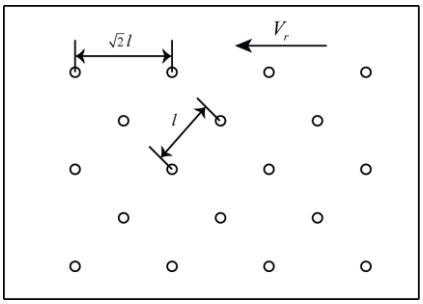

Figure 7 Schematic of raindrop distribution

The duration of raindrop moving over 1 m is $1/V_r$, and during this period the momentum of raindrops with the diameter of D is

$$M_r(V_r,D,R)=F_{peak}(V_r,D)S(V_r,R)n(D,R) \tag{9}$$

where $S(V_r, R)$ denotes the area of the normalized curve in Figure 6 integrating from 0 to the time of Δt.

And then the rain pressure for the specified diameter of D is derived as follows:

$$P_{rain}(V_a,R,D,H,\alpha)=\frac{M_r(V_r,D,R)}{1/V_r}$$
$$=k\rho_w S(\gamma(H,D,\alpha)V_a,R)n(D,R)\gamma^3(H,D,\alpha)V_a{}^3D^3 \quad (10)$$

The front and rear areas of the tower impinged by the raindrops for a specific rainfall are discrete, so the impinging area is $2A$ [7]. Consequently the rain load is derived as [6]

$$F_{rain}(V_a,R,H,\alpha,A)=2\int_0^\infty P_{rain}(V_{10},R,D,H,\alpha)A\,dD \quad (11)$$

The aeroelastic tower model adopted herein in the wind tunnel test for validating the proposed rain load model is made of copper and fabricated as shown in Figure 8 [8]. Plastic pipes and plates are used to simulate the aerodynamic property of tower bars. The artificial rainfall device as shown in Figure 9 is composed of multiple nozzles.

Figure 8 Aeroelastic model of transmission tower

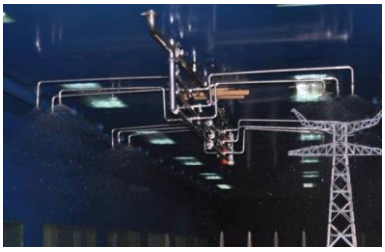

Figure 9 Artificial rainfall device

Comparisons of the RMS accelerations and the percentages between the numerical simulation and wind tunnel test are illustrated in Figure 10 and Figure 11, respectively. From Figure 10, it can be seen that most of the numerical results are very close to experimental ones and the maximum relative errors only reach to 9.00%, which illustrates that using the proposed method to calculate the rain load is generally reliable.

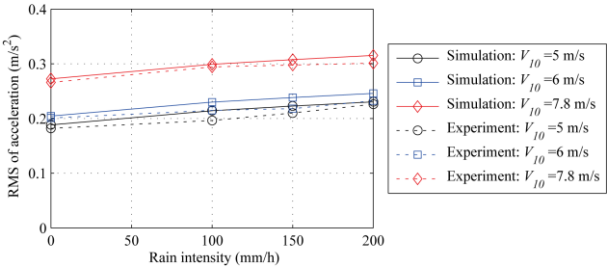

Figure 10 Comparison of RMS acceleration between numerical simulation and wind tunnel test

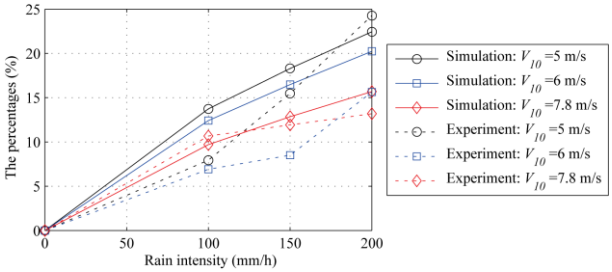

Figure 11 Comparison of percentages between numerical simulation and wind tunnel test

Rain load for transmission line

Except the raindrop impinging force, the rainfall also has an important effect on the aerodynamic property of transmission conductor. The surface roughness has a great impact on the aerodynamic property of circular cylinder. In the ESDU [4] the curves of drag coefficient vs. Reynolds number under different surface conditions are presented and the schematic curves are illustrated in Figure 12 to clarify the mechanism of rainfall on the aerodynamic property of transmission conductor. As can be seen in Figure 12, the subcritical stage moves to the right and the other three stages move to the lower right with the surface of circular cylinder becoming smooth.

The transmission conductor is made up of many strands of circular steel wire, and there are many grooves in the conductor surface. When it rains, the conductor surface will be covered with water which can be filled in the grooves, and the conductor surface becomes smooth. Based on the theory of flow around a circular cylinder, it is known that the aerodynamic property of water-covered conductor will be very different.

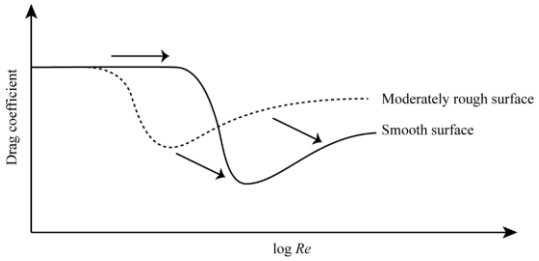

Figure 12 Effect of surface roughness on the aerodynamic property of circular cylinder [4]

The potential loads acting on the transmission conductor under wind and rain excitations are drawn in Figure 13.

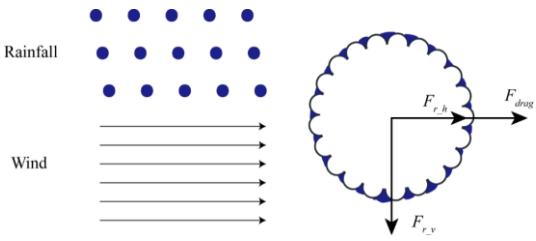

Figure 13 Schematic of potential loads acting on transmission conductor

In Figure 13, F_{r_h} and F_{r_v} denote the horizontal and vertical raindrop impinging forces, respectively, and F_{drag} denotes the wind force acting on the conductor. The horizontal load F_{total_h} is composed of F_{r_h} and F_{drag} [5]:

$$F_{total\_h}=F_{r\_h}+F_{drag}$$
$$=\int_0^\infty P_{rain}(V_a,R,D,H,\alpha)AdD+\frac{\rho_a V_a^2}{2}C_D(V_a,R)A \quad (12)$$

where $C_D(V_a, R)$ is the drag coefficient of transmission conductor under both wind and rain excitations.

As far as we know, no standard refers to the rain load, let alone the effect of rainfall on the drag coefficient of transmission conductor. Therefore, it's urgent to conduct the relevant experiments to determine $C_D(V_a, R)$.

The vertical load F_{r_v} is expressed as follows:

$$F_{total\_v} = F_{r\_v} = \int_0^{\infty} P_{rain}(V_{term}(D), R, D) A dD \qquad (13)$$

Kikuchi et al. [9] performed the measurement of aerodynamic drag of new-design electric power wire in a heavy rainfall and wind, and the experimental results were used in this paper to study the aerodynamic influence of rainfall on the tower-line system.

A FEM of tower-line system, which includes three towers and four spans of conductors, is established as shown in Figure 14 to study the effect of rainfall on the tower response.

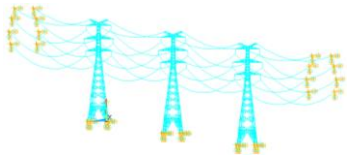

Figure 14 The FEM of transmission tower-line system

The average displacements for different combinations of basic wind speed and rain intensity are listed in Table 1, which can be derived that the heavier rain intensity results in the larger displacement except for the basic wind speed of 15 m/s. In addition, the increasing percentages of displacement induced by the rain loads relative to the wind loads are calculated and illustrated in Figure 15, in which the maximum percentage of displacement reaches to 22.00%, demonstrating that the influence of rain load on the response of tower-line system is important.

V_{10} (m/s) / R (mm/h)	15	20	25	30
0	0.108	0.155	0.230	0.322
150	0.104	0.181	0.274	0.374
240	0.110	0.189	0.276	0.385

Table 1 The average tower tip displacement (unit: m)

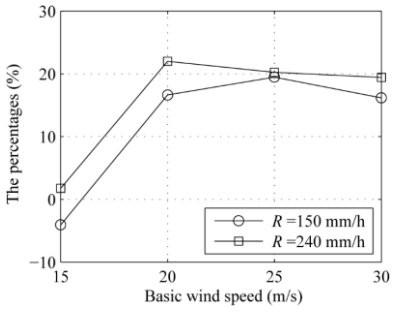

Figure 15 The increasing percentages of displacement induced by the rain load relative to the wind load

Conclusions

The mechanism of rain load for the tower-line system is preliminarily revealed, which includes both the raindrop impinging force and the change of aerodynamic force. For the transmission tower, the heavier rain intensity results in the larger displacement except for the basic wind speed of 15 m/s, and the maximum percentage of displacement can reach to 22.00%, indicating that the rain load has great influence on the dynamic vibration of tower-line system and cannot be ignored.

Acknowledgments

This research was supported by the National Natural Science Foundation of China (Grant No. 51421064) and the Fundamental Research Funds for the Central Universities (DUT17RC(3)007).

References

[1] Blocken, B., 50 years of Computational Wind Engineering: Past, present and future. *Journal of Wind Engineering and Industrial Aerodynamics*, **129**, 2014, 69-102.

[2] Choi, E.C., Numerical modelling of gust effect on wind-driven rain. *Journal of Wind Engineering and Industrial Aerodynamics*, **72**, 1997, 107-116.

[3] Choi, E.C., Wind-driven rain and driving rain coefficient during thunderstorms and non-thunderstorms. *Journal of wind engineering and industrial aerodynamics*, **89**, 2001, 293-308.

[4] ESDU, 1980. Mean forces, pressures and flow field velocities for circular cylindrical structures: single cylinder with two-dimensional flow. Engineering Sciences Data Unit, London.

[5] Fu, X., Li, H.-N., Dynamic analysis of transmission tower-line system subjected to wind and rain loads. *Journal of Wind Engineering and Industrial Aerodynamics*, **157**, 2016, 95-103.

[6] Fu, X., Li, H.-N., Yang, Y.B., Calculation of rain load based on single raindrop impinging experiment and applications. *Journal of Wind Engineering and Industrial Aerodynamics*, **147**, 2015, 85-94.

[7] Fu, X., Li, H.-N., Yi, T.-H., Research on motion of wind-driven rain and rain load acting on transmission tower. *Journal of Wind Engineering and Industrial Aerodynamics*, **139**, 2015, 27-36.

[8] Fu, X., Lin, Y.-X., Li, H.-N., Wind tunnel test and response analysis of high-voltage transmission tower subjected to combined loads of wind and rain. *Engineering Mechanics*, **34**, 2014, 72-78.

[9] Kikuchi, N., Matsuzaki, Y., Yukino, T., Ishida, H., Aerodynamic drag of new-design electric power wire in a heavy rainfall and wind. *Journal of Wind Engineering and Industrial Aerodynamics*, **91**, 2003, 41-51.

[10]Li, H.-N., Tang, S.-Y., Yi, T.-H., Wind-rain-induced vibration test and analytical method of high-voltage transmission tower. *Structural Engineering and Mechanics*, **48**, 2013, 435-453.

[11]Tabatabai, M., Krishnasamy, S., Meale, J., Cooper, K., Response of smooth body, trapezoidal wire overhead (compact) conductors to wind loading. *Journal of Wind Engineering and Industrial Aerodynamics*, **41**, 1992, 825-834.

[12]Wardlaw, R., Cooper, K., Ko, R., Watts, J., Wind tunnel and analytical investigations into the aeroelastic behaviour of bundled conductors. *Power Apparatus and Systems, IEEE Transactions on*, **94**, 1975, 642-654.

[13]Xie, Q., Sun, Q., Guan, Z., Zhou, Y., Wind tunnel test on global drag coefficients of multi-bundled conductors. *Journal of Wind Engineering and Industrial Aerodynamics*, **120**, 2013, 9-18.